厚生労働科学研究費補助金（循環器疾患等生活習慣病対策総合研究事業）
分担研究報告書

弓部大動脈全置換術における超低体温療法と中等度低体温療法における血小板機能の比較検討

分担研究者　宮田茂樹　国立循環器病センター輸血管理室医長

研究要旨；従来までの超低体温を用いた弓部全置換術に比較して、生理的条件に近付けた28℃中等度低体温下手術では、（超）低体温の弊害である体外循環時間の延長、臓器の温度較差、非生理的環境、それに基づく全身浮腫、肺障害、出血傾向などが回避でき、早期回復や出血が少ないなど「warm surgery」の利点が期待できうる。本研究では、中等度低体温下弓部全置換術と超低体温下弓部全置換術、それぞれの手術における血小板数、血小板機能の推移を測定し、輸血量との関連を含めた解析を行うことにより、低体温の血小板機能に与えるインパクトを検討した。

血小板機能の測定系として、平行板型フローチャンバーを用いたずり応力下血小板機能評価法を用い、低体温が血小板機能に与える影響について検討するとともに、血小板数の推移ならびに輸血量を超低体温（20℃）と中等度低体温（28℃）で比較検討した。結果として、現時点で、いまだすべての症例報告書の回収、データ固定が行われていない段階ではあるが、28℃中等度低体温下手術群で、すべての血液製剤（赤血球製剤、新鮮凍結血漿、濃厚血小板製剤）の輸血量が少なかった。術前、人工心肺離脱直後で血小板輸血実施前の血小板数、血小板機能を両群で比較した場合、血小板数の推移は、超低体温（20℃）で、術前207,780/μl から、人工心肺離脱直後で血小板輸血実施前には、88,000/μl まで低下していた。一方、中等度低体温（28℃）弓部全置換術群では、200,960/μl から、78,000/μl までの低下であり、血小板数の減少割合はほぼ同様であった。一方、血小板機能で見てみると、超低体温群で、血小板血栓の高さは、術前22.8μmから人工心肺離脱直後で血小板輸血実施前に5.8μmへ、表面占有率は、65.3%から20.6%への低下であったが、中等度低体温弓部全置換術群では、血小板血栓の高さは、術前18.9μmから人工心肺離脱直後で血小板輸血実施前に5.6μmへ、表面占有率は、54.2%から21.9%への低下であり、中等度低体温（28℃）弓部全置換術群で若干血小板機能低下割合が少ない（特に表面占有率において）傾向となっていた。

しかしながら、このような体温の違いによる若干の血小板機能の相違だけで、観察されたようなすべての製剤における輸血量の明らかな相違を説明することは困難であり、血小板機能以外の凝固線溶系、炎症など他の因子が複雑に関与している可能性が示唆された。

現時点で、登録された患者数が少なく、解析可能な患者数が限られているため、明確ではないが、中等度低体温では、人工心肺中の血小板に対する環境として、超低体温より有利に働き、血小板数ならびに血小板機能が保護され、出血量が少なく、止血効果が良好となる可能性があることが示唆された。

A. 研究目的

近年、高齢化が進み、大動脈疾患に対する手術件数は冠動脈手術と共に増加の一途をたどっている。しかしながら、通常の開心術に比べ、高い手術侵襲度、手術の困難さ、患者の高齢化、多岐にわたる併存疾患、大量出血などの問題があり、その手術成績の向上は急務である。特に、弓部大動脈瘤に対する人工血管置換術（弓部全置換術）はその中心をなし、生命予後に止まらず、高次機能を含め脳保護法は未だに重要な課題である。我が国では、脳保護法として、従来からの超低体温循環停止に加え、補助手段として選択的順行性

脳灌流（SCP）と逆行性脳灌流（RCP）が開発され臨床応用されてきた。最近では、時間的制約の少ない点から、より生理的なSCPが定着し広く用いられている。このSCPを用いた場合、脳の灌流が維持されており、必ずしも超低体温を用いる必要がない。その観点から、最近になり生理的条件に近付けた28℃中等度低体温下手術が試みられ、有効性が報告されつつある。弓部全置換術においても、通常の開心術の進歩、発展と同様に、（超）低体温の弊害である体外循環時間の延長、臓器の温度較差、非生理的環境、それに基づく全身浮腫、肺障害、出血傾向などが回避でき、早期回復や出血が少ないなど「warm surgery」の利点が期待できうる。しかしながら、現在までの報告では、比較対照群がない単独での報告で多く、従来からの超低体温下弓部全置換と比べどの程度の有用性、安全性があるかは明確にされていない。中等度低体温下手術の有効性を明らかにするためには、従来からの超低体温下弓部全置換との厳密な比較検討が必要とされる。本研究では、中等度低体温下弓部全置換術と超低体温下弓部全置換術における多施設共同前向き調査研究の一環として、中等度低体温下弓部全置換術と超低体温下弓部全置換術それぞれの手術における血小板数、血小板機能の推移を測定し、輸血量との関連を含めた解析を行うことにより、低体温の血小板機能に与えるインパクトを検討することとした。

弓部全置換術の場合、人工心肺を必要とすることで血小板機能低下が起こる事が指摘されている。また、血小板機能に体温が与える影響についても指摘されている。また、ヘパリン、プロタミンを使用する等で、血小板機能が損なわれるという報告も存在する。したがって、本研究では、血小板数だけでなく、血小板機能に関する評価を行った。近年、血小板機能を評価する場合に、生体内で血小板が存在する環境である流動状況下での血小板機能を考慮する必要性が指摘され、ずり応力下血小板機能評価の新しい概念が確立されつつある。生理的条件に近い系として、体温が血小板機能に与える影響を *ex vivo* で、血小板膜レセプターと各種粘着蛋白との相互作用を含めた詳細な評価が可能となる。本研究では、平行板型フローチャンバーを用いたずり応力下血小板機能評価系にて、低体温が血小板機能に与える影響について検討した。

B. 研究方法

1） ずり応力下血小板機能測定

術直前、人工心肺離脱直後（血小板輸血を実施する前）、ならびに手術翌朝に、抗凝固剤として選択的抗トロンビン剤であるアルガトロバンを終濃度125 μg/mlとなるよう添加し採血した検体を用いて検討した。採血した全血をコラーゲンType Iを固相化したガラスプレートを組み込んだ平行板型フローチャンバー内に、血小板を蛍光色素（メパクリン）で標識して流し込み、高ずり応力(2000/s)のかかる部位でのコラーゲン固相表面上での血小板血栓形成過程を倒立型蛍光顕微鏡でリアルタイムに観察した。また、これらの画像をCCDカメラによりコンピュータに取り込みデジタル化し、画像解析を行った。測定開始10分後に形成された血小板血栓をZ方向にスキャンすることにより血小板血栓の3次元イメージを再構築し、血小板血栓の高さを測定した。加えて血小板血栓の表面占有率（測定視野全体面積に対する血小板血栓の占める割合）を測定し、この2つを血小板機能の指標とした。血小板血栓の表面占有率は主に、von Willebrand factorと血小板膜糖蛋白GPIb/IX/V 複合体との反応に依存する血小板粘着能を表し、血小板血栓の高さは、von Willebrand factor, fibrinogenなどの粘着蛋白と血小板膜蛋白GP IIb/IIIaとの反応に依存した血小板凝集能を評価することとなる。

2） 血小板数並びに術中輸血量

周術期の血小板数の推移ならびに輸血量（赤血球製剤、新鮮凍結血漿、血小板製剤）を超低体温と中等度低体温で比較検討した。

（倫理面への配慮）

本研究は、参加各施設における倫理委員会の承認

を受けた上で、患者からの文書による同意を得て行った。

C. 研究結果

1) ずり応力下血小板機能測定

超低体温（20℃）を用いて弓部全置換術を行った患者で、国立循環器病センターのサブスタディーとして解析可能であった症例における術前、人工心肺離脱直後（血小板輸血実施前）、術翌朝における検体を平行板型フローチャンバー内に流し込み解析をおこなった。術前（n=18）における測定開始10分後の血小板血栓の高さは、22.8（平均）±7.5（1 S.D.）μmで、表面占有率は65.3（平均）±17.7（1 S.D.）%あった。人工心肺離脱直後で血小板輸血実施前（n=15）の測定開始10分後の血小板血栓の高さは5.79（平均）±0.92（1 S.D.）μmで、表面占有率は20.6（平均）±7.9（1 S.D.）%あった。術翌朝（n=9）における測定開始10分後の血小板血栓の高さは、21.6（平均）±7.9（1 S.D.）μmで、表面占有率は56.4（平均）±20.0（1 S.D.）%あった。一方、中等度低体温（28℃）を用いて弓部全置換術を行った患者における結果は下記のとおりであった。術前（n=18）における測定開始10分後の血小板血栓の高さは、18.9（平均）±10.3（1 S.D.）μmで、表面占有率は54.2（平均）±21.1（1 S.D.）%であった。人工心肺離脱直後で血小板輸血実施前（n=15）の測定開始10分後の血小板血栓の高さは5.56（平均）±0.68（1 S.D.）μmで、表面占有率は21.9（平均）±7.5（1 S.D.）%であった。術翌朝（n=9）における測定開始10分後の血小板血栓の高さは、11.0（平均）±8.1（1 S.D.）μmで、表面占有率は39.1（平均）±20.8（1 S.D.）%であった。いずれの群においても、術前と比較して人工心肺離脱直後に明らかな血小板機能低下が認められ、術翌日には改善していた。現時点では、いまだすべての症例報告書の回収、データ固定が行われていない段階であるが、中等度低体温（28℃）患者群で、術前の血小板機能が若干低く、人工心肺離脱直後で血小板輸血実施前では、両群にほとんど差が無く、術翌日では中等度低体温患者群の方が、血小板機能が低い傾向が認められた。

2) 血小板数ならびに術中輸血量

超低体温（20℃）を用いて弓部全置換術を行った患者での血小板数の推移は、術前（n=27）は207,780（平均）± 44,290（1 S.D.）/μl、人工心肺離脱直後で血小板輸血実施前（n=24）は88,000（平均）± 57,990（1 S.D.）/μl、術後（n=27）は119,360（平均）± 47,080（1 S.D.）/μlであった。一方、中等度低体温（28℃）を用いて弓部全置換術を行った患者における血小板数の推移は、術前（n=25）は200,960（平均）± 47,220（1 S.D.）/μl、人工心肺離脱直後で血小板輸血実施前（n=23）は78,000（平均）± 62,610（1 S.D.）/μl、術後（n=24）は69,020（平均）± 50,880（1 S.D.）/μlであった。現時点で、いまだすべての症例報告書の回収、データ固定が行われていない段階であるが、両群間で、術前、人工心肺離脱直後で血小板輸血実施前での血小板数にはそれほど大きな差は認められなかった。一方、術後の血小板数は、中等度低体温群で超低体温群と比較して低かった。

輸血量について検討してみると、超低体温（20℃）を用いて弓部全置換術を行った患者（n=27）では、赤血球製剤は、14.4単位 ±11.7 単位、新鮮凍結血漿17.0単位 ± 11.2 単位、濃厚血小板製剤21.6単位 ± 20.2単位であった。一方、中等度低体温（28℃）を用いて弓部全置換術を行った患者(n=25)では、赤血球製剤5.4単位 ±7.0単位、新鮮凍結血漿6.3単位 ± 7.8 単位、濃厚血小板製剤4.0単位 ±10.4単位であった。いまだすべての症例報告書の回収、データ固定が行われていない段階であるが、赤血球製剤、新鮮凍結血漿、濃厚血小板製剤、いずれの製剤においても輸血量は、中等度低体温群で少なかった。

超低体温群において、中等度低体温群と比較して術翌日の血小板機能が高く、術後血小板数が多かったのは、血小板製剤輸血量が超低体温（20℃）群で多かったことの影響であると考えられた。

D. 考案

従来までの超低体温を用いた弓部全置換術に

比較して、生理的条件に近付けた28℃中等度低体温下手術では、(超) 低体温の弊害である体外循環時間の延長、臓器の温度較差、非生理的環境、それに基づく全身浮腫、肺障害、出血傾向などが回避でき、早期回復や出血が少ないなど「warm surgery」の利点が期待できうる。

本研究では、中等度低体温下弓部全置換術と超低体温下弓部全置換術、それぞれの手術における血小板数、血小板機能の推移を測定し、輸血量との関連を含めた解析を行うことにより、低体温の血小板機能、止血機能に与えるインパクトを検討した。現時点で、いまだすべての症例報告書の回収、データ固定が行われていない段階で、それぞれのデータの相関等、詳細な検討を行っておらず、断定的な結論を導くことは困難であるが、生理的条件に近付けた28℃中等度低体温下手術にて、すべての血液製剤 (赤血球製剤、新鮮凍結血漿、濃厚血小板製剤) の輸血量が少なかった。術前、人工心肺離脱直後で血小板輸血実施前の血小板数、血小板機能を両群で比較した場合、血小板数の推移は、超低体温 (20℃) で、術前 207,780/μl (平均) から、人工心肺離脱直後で血小板輸血実施前には、88,000/μl (平均) まで低下していた。一方、中等度低体温 (28℃) 弓部全置換術群では、200,960/μl (平均) から、78,000/μl (平均) までの低下であり、血小板数の減少割合はほぼ同様であった。一方、血小板機能で見てみると、超低体温群で、血小板血栓の高さは、術前 22.8μm から人工心肺離脱直後で血小板輸血実施前に 5.8μm へ、表面占有率は、65.3%から 20.6%への低下であったが、中等度低体温弓部全置換術群では、血小板血栓の高さは、術前 18.9μm から人工心肺離脱直後で血小板輸血実施前に5.6μmへ、表面占有率は、54.2%から 21.9%への低下であり、中等度低体温 (28℃) 弓部全置換術群で若干血小板機能低下割合が少ない (特に表面占有率において) 傾向となっていた。しかしながら、このような体温の違いによる若干の血小板機能の相違だけで、観察されたようなすべての製剤における輸血量の明らかな相違を説明することは困難であり、血小板機能以外の凝固線溶系、炎症など他の因子が複雑に関与している可能性が高いと考えられる。

現時点では、いまだすべての症例報告書の回収、データ固定が行われていない。また、それぞれのデータの相関等、詳細な検討を行っていない段階であり、今後、中等度低体温 (28℃) 弓部全置換術において輸血量が少ない因子について、さらに詳細な検討を加えていく必要があると考えられた。

E. 結論

- 最終的な解析結果ではないものの、中等度低体温 (28℃) 弓部全置換術群では、超低体温 (20℃) 群と比較して、輸血量が少ない傾向が見られた。低体温による血小板機能低下が、中等度低体温では超低体温と比較して軽減されている可能性が示唆された。しかしながら、それ以外の因子 (凝固線溶系、炎症など) が輸血量の変化に対してより強く関与していることが示唆された。

F. 健康危険情報

特になし

G. 関連する研究発表

1. 学会発表

1) 宮田茂樹: 小児開心術における輸血トリガー値の予後に与える影響についての考察. 第 42 回小児循環器学会総会. 名古屋、2006.
2) 亀井政孝、宮田茂樹、畔政和:人工心肺による血小板機能障害とその対策. 第 11 回日本心臓血管麻酔学会学術大会. 長崎、2006.
3) 宮田茂樹、亀井政孝、山本賢、角谷勇実、阪田敏幸、佐野隆宏、半田誠、八木原俊克:心臓血管外科手術における血小板輸血が必要となる危険因子. 第50回日本輸血学会近畿支部会総会. 大阪、2006.

2. 論文発表

1) 宮田茂樹: 外科周術期輸血トリガー値に関する考察. 別冊・医学のあゆみ 輸血医療・医学の新

展開. 山口一成 編 医歯薬出版株式会社 2006; 218(6):585-592.
中谷武嗣、宮田茂樹:人工弁・補助循環における抗血小板療法. 抗血小板療法の新しい使い方. 内山真一郎、堀正二 編. 医薬ジャーナル社 2006; 153-158.

H. 知的財産権の出願・登録状況(予定を含む)

本研究課題に関連する当該事項の登録はない。

厚生労働科学研究補助金（循環器疾患等生活習慣病対策総合研究事業）
分担研究報告書

弓部大動脈全置換術における超低体温療法と中等度低体温療法のランダム化比較試験に関する研究：弓部大動脈全置換術における超低体温療法の中等度低体温療法の多施設共同前向き調査研究

荻野　均　　湊谷　謙司
松田　均　　佐々木　啓明　　八木原　俊克

研究要旨；中等度低体温下弓部大動脈全置換術と超低体温下同手術の多施設共同前向き比較研究を行った。本年度は、ランダム化比較試験に先立ち二群間のデータを前向きに蓄積することを目的とした。当施設では合計31例の症例を登録し、研究プロトコールに則り臨床研究を施行した。7例で有害事象を認めたが、有害事象は研究との因果関係を認めなかった。現時点において未だ統計処理中のデータが多く、部分的に報告することは憚られるが、基本的には中等度低体温法の有用性や安全性を裏付けるデータとなり、次段階のランダム化比較試験へ向けての準備は整ったと考える。

A. 研究目的

弓部全置換術は、様々な脳保護手段が開発され、著しい成績の向上をみた。しかし、いずれの方法も 20℃以下の超低体温の不利な条件下に成立している。一方、生理的灌流である SCP 下では必ずしも超低体温を用いる必要がなく、最近では28℃中等度低体温下手術が試みられている。しかし、超低体温下手術と中等度低体温下手術を厳密に比較した報告は未だない。本研究は、厳密な二群間のランダム化比較試験に向けて、28℃中等度低体温と 20℃超低体温における多施設共同前向き調査研究を行い、それぞれの弓部全置換術の特徴を明らかにしようとするものである。

B. 研究方法

SCP を脳保護手段とした弓部全置換術において、28℃中等度低体温と 20℃超低体温における多施設共同前向き調査研究を行い、各々の特徴を明らかにする。手術は、胸骨正中切開下に SCP を脳保護手段として、4分枝人工血管を用いた弓部分枝個別再建法により弓部全置換を行った。各群の SCP 圧、SCP 量は① 膀胱温 20℃ SCP 圧 30-50 mmHg → 10 ml/kg/min、② 膀胱温 28℃ SCP 圧 ≧50 mmHg → 15～25 ml/kg/min。評価項目は、1) 術後 30 日以内死亡、および脳・脊髄障害、心臓障害、肺障害、腎障害、出血、感染、などの合併症の発生割合、および2) 臨床データ：① 手術方法 ②出血量 ③循環動態計測 ④呼吸状態 ⑤脳神経機能 ⑥腎機能、肝機能 ⑦凝固機能 ⑧その他

C. 研究結果・考察

本研究は 2 月末から開始され、最終的に本院では 31 例の症例登録がなされた。7 例で有害事象を

認めた。このうち、心不全が２例、呼吸不全が２例、脳神経障害が２例、出血が１例であった。心不全の１例が多臓器不全に陥り死亡し、脳神経障害の１例に後遺症を残したが、残る５例は軽快した。いずれも研究との因果関係は無し、あるいは不明であった。現時点において未だデータは統計処理中であるが、それぞれの弓部全置換術の特徴は少なくとも明らかにされたと考える。すなわち、中等度低体温群で死亡、合併症を含めた有害事象の発生頻度が低く、輸血量も少なく、人工呼吸管理も短い傾向が示唆された。

D. 結論

基本的には中等度低体温法の有用性や安全性を裏付けるデータとなり、これら中等度低体温下手術の利点を主要項目として設定することとし、二群間でのランダム化比較試験へ向けての準備は整ったと考える。

E. 健康危険情報

特になし。

G. 研究発表

1. 論文発表

1) Ogino H, Ando M, Sasaki H, Minatoya K: Total arch replacement using a stepwise distal anastomosis for arch aneurysms with distal extension. Eur J Cardiothorac Surg, 29(2):255-7,2006

2) Minatoya K, Ogino H, Matsuda H, Sasaki H, Yagihara T, Kitamura S: Surgical management of distal arch aneurysm : another approach with improved results. Ann Thorac Surg, 81(4) : 1356-7,2006

3) Sasaki H, Ogino H, Matsuda H, Minatoya K, Ando M, Kitamura S: Intergraded total arch replacement using selective cerebral perfusion: a six-year experience. Ann Thorac Surg, in press, 83(2): S805-10,2007

2. 学会発表

1) Ogino H, Minatoya K, Matsuda H, Sasaki H, Ando M, Kitamura S: Evolving surgery for acute A aortic dissection using selective cerebral perfusion and with aggressive total arch repair. American Heart Association. 2006

2) Sasaki H, Ogino H, Matsuda H, Minatoya K, Ando M, Kitamura S: Integrated total arch replacement using selective cerebral perfusion: Six years' experience. Aortic Surgery Symposium.2006

H. 知的財産権の出願・登録状況（予定を含む）

本研究課題に関連する当該事項の登録はない。

厚生労働科学研究補助金（循環器疾患等生活習慣病対策総合研究事業）
分担研究報告書

弓部大動脈全置換術における超低体温療法と中等度低体温療法のランダム化比較試験に関する研究
研究デザインに関する研究

分担研究者　　国立循環器病センター研究所病因部室員　嘉田　晃子

研究要旨；28℃中等度低体温下弓部全置換術と 20℃超低体温下弓部全置換術の多施設共同前向き調査研究の症例登録が終了した。術後 3 週までのデータの集計より、多施設共同ランダム化比較試験の研究計画を検討した。主要評価項目として輸血量を設定し、独立したデータ安全性評価委員会を設け、安全性と評価項目の妥当性を確認することとした。

A. 研究目的

28℃中等度低体温下弓部全置換術と 20℃超低体温下弓部全置換術について、適切なデザインの研究によりそれらの特徴を明らかにし、有効性や安全性を評価することが重要である。そのために、多施設共同前向き調査研究を適切に実施し、その評価をもとに、多施設共同ランダム化比較試験の研究計画を検討する。

B. 研究方法

多施設共同前向き調査研究の進捗を管理する。症例登録が終了した後、術後 3 週までのデータの集計し、多施設共同ランダム化比較試験の研究計画を検討する。

（倫理面への配慮）

前向き調査研究およびランダム化比較試験は、ヘルシンキ宣言、および臨床研究に関する倫理指針に従い実施する。データを解析する際には個人情報の取り扱いに留意する。

C. 研究結果

前向き調査研究は、2006 年 12 月に被験者登録を終了した。5 施設から症例が登録され、術後 3 週までの症例報告書が回収された 52 例について集計を行った。

その結果、輸血量、術後 30 日以内の合併症の発生、人工呼吸管理時間などに 28℃群と 20℃群による特徴が見られた。

これらをもとに、ランダム化比較試験の研究計画を検討した。

対象集団について、主に安全性と評価可能性を考慮し、前向き調査研究より詳細に選択・除外基準を設定した。

選択基準：

(1)弓部全置換術単独の患者（解離症例を含む）

(2)80 歳未満の患者

(3)弓部～遠位弓部瘤で下行大動脈への伸展が少なく正中到達が可能な患者

除外基準：

(1)緊急患者（大動脈瘤破裂、急性大動脈解離など）

(2)広範囲大動脈病変：手術適応に近い大動脈基部、

下行大動脈（正中から到達困難なもの）、胸腹部大動脈、腹部大動脈瘤病変を合併する患者
(3)上行、弓部、弓部分枝に著しい粥状硬化性病変を有する患者
(4)高安病、Behcet病、Marfan症候群、Ehlers-Danlos症候群などの特殊大動脈病変患者
(5)重症閉塞性動脈硬化症合併患者
(6)再手術（再胸骨正中切開）患者
(7)脳、心、肺、肝、腎、血液・凝固機能に中等度以上の異常（合併疾患）を認める患者
(8)感染所見のある患者
(9)担癌患者
(10)痴呆（認知症）、精神疾患患者
(11)その他、担当医師が不適当と判断した患者

主要評価項目は、輸血量(MAP＋FFP)とした。副次的評価項目として、術後 30 日以内死亡（手術死亡）、および脳・脊髄障害、心臓障害、肺障害、腎障害、出血、感染などの合併症の発生割合を設定した。さらに、その他の評価項目として、血小板輸血を行った症例の割合、無輸血症例の割合、死亡および副次的評価項目の各合併症の発生割合、人工呼吸管理時間（抜管時期）などを評価する予定である。

症例数は、前向き調査研究をもとに主要評価項目から設定し、1 群 50 例、合計 100 例を目標とする。

また、第三者の委員によるデータ安全性評価委員会を設置する。委員会は、登録開始後５ヶ月、登録終了後、及び追跡終了後に開催し、安全性と評価項目の妥当性を確認する。

D. 考察

28℃中等度低体温下弓部全置換術と 20℃超低体温下弓部全置換術の特徴を明らかにするための評価項目は未だ確立されていない。本研究グループでは、前向き調査研究で得られた情報をもとに評価項目を設定し、ランダム化比較試験で評価していく予定であり、独立に設けたデータ安全性評価委員会の役割は重要である。

また、確かなエビデンスを示していくためにはデータマネジメントが大切である。クリニカル・データマネジメントは、研究データを統一して評価できる情報にまとめることであり、研究の計画段階から最終の報告書が完成するまでの各段階でおこなわれる。本研究では、前向き調査研究とランダム化比較試験でほぼ同様の手順で登録、症例報告書の収集、管理を行っていく予定であり、各実施医療機関、事務局、データセンターが協力して効率的に進めていきたい。

E. 結論

28℃中等度低体温下弓部全置換術と 20℃超低体温下弓部全置換術の多施設共同前向き調査研究の症例登録が終了し、術後 3 週までのデータの集計より、多施設共同ランダム化比較試験の研究計画を検討した。主要評価項目として輸血量を設定し、独立したデータ安全性評価委員会を設け、安全性と評価項目の妥当性を確認していくこととした。

F. 健康危険情報

特になし。

G. 研究発表

本研究課題に関連する今年度の研究発表はない。

H. 知的財産権の出願・登録状況（予定を含む）

本研究課題に関連する当該事項の登録はない。

III. 研究成果の刊行物・別刷

ELSEVIER

European Journal of Cardio-thoracic Surgery 29 (2006) 255–257

EUROPEAN JOURNAL OF CARDIO-THORACIC SURGERY

www.elsevier.com/locate/ejcts

How-to-do-it

Total arch replacement using a stepwise distal anastomosis for arch aneurysms with distal extension☆

Hitoshi Ogino[a,*], Motomi Ando[b], Hiroaki Sasaki[a], Kenji Minatoya[a]

[a] Department of Cardiovascular Surgery, National Cardiovascular Center, 5-7-1 Fujishirodai, Suita, Osaka 565-8565, Japan
[b] Department of Thoracic Surgery, Fujita Health University, Mizukake-cho, Toyoake, Aichi 470-1192, Japan

Received 2 August 2005; received in revised form 17 October 2005; accepted 19 October 2005

Abstract

A total of 120 patients having arch to distal arch aneurysm with downstream extension underwent total arch replacement, with individual arch-vessel reconstruction through median sternotomy using a novel 'stepwise' distal aortic anastomosis. Cardiopulmonary bypass was established by cannulating the right axillary artery and the ascending aorta or femoral artery. Hypothermia was at 22–28 °C. Through the aneurysm, the descending aorta was divided. Distal anastomosis using the stepwise technique was performed; a tube graft of length 7–12 cm was inserted into the descending aorta and anastomosed by running suture. The distal end of the inserted graft was extracted, and a further four-branched arch graft was joined to it. Selective cerebral perfusion was used for cerebral safety during arch repair. There were three hospital deaths (2.5%). Two patients (1.7%) developed permanent neurological dysfunction and three patients (2.5%) suffered transient cerebral deficits. Three patients (2.5%) required reentry for postoperative bleeding although in none of them bleeding was from the distal anastomosis site with the stepwise technique. Stepwise anastomosis is a useful and secure alternative for distal anastomosis in total arch replacement for arch to distal arch aneurysms with distal extension.

Keywords: Aortic arch; Aneurysm; Aortic dissection; Aortic surgery

1. Introduction

For arch to distal arch aneurysms, it is not agreed whether a median or lateral approach is better, particularly for aneurysms with distal extension [1–7]. The median approach aims to provide cerebral and cardiac safety [1–4]. However, the distal anastomosis is often difficult and bleeding from it is a serious problem [6,7]. We have therefore used a novel stepwise technique providing a technically easy and secure anastomosis.

2. Patients and methods

Between 1999 and 2003, 120 patients (74 years old) having an arch to distal arch aneurysm underwent total arch replacement. Of these, 112 patients had non-dissecting and two had dissecting aneurysms. The other six had a combined pathology. Ten patients required emergency surgery.

The aneurysm was approached through median sternotomy (Fig. 1A). After full heparinization, a 10–16 Fr straight thin-wall cannula was inserted into the right axillary artery (RAxA) on the right armpit [8]. Cardiopulmonary bypass (CPB) was established by cannulation involving also the femoral artery or the ascending aorta. The patients were cooled to 22–28 °C. Following hypothermic circulatory arrest, selective cerebral perfusion (SCP) was begun through the RAxA perfusion by clamping the brachiocephalic artery (BCA). The arch was opened and a 12 Fr SCP balloon cannula was inserted into the left common carotid artery (LCCA) (Fig. 1B). In recent series with moderate hypothermia at 25–28 °C, the left subclavian artery (LSCA) was also perfused. With SCP, the descending aorta was divided through the aneurysm. Distal aortic anastomosis was done using a stepwise technique. First, an invaginated tube graft of length 7–12 cm (a piece of the quadrifurcated arch graft) was inserted into the descending aorta (Fig. 1C). The position of the proximal end of the invaginated graft was adjusted to match the level of the divided end of the descending aorta. The anastomosis was then easy to perform, with a good surgical view, using an over and over running suture of 3-0 or 4-0 polypropylene, with reinforcement by Teflon felt strip (Fig. 2A). The distal end of the inserted graft was extracted proximally. For arch reconstruction, a further four-branched arch graft was attached to this stepwise graft using a running 3-0 polypropylene suture (Fig. 2B). Antegrade aortic perfusion was initiated. The LSCA was reconstructed with a branch graft.

☆ This paper was presented in the Aortic Surgery Symposium VI in New York in 2004.

* Corresponding author. Tel. +81 6 6833 5012; fax: +81 6 6872 7486.
E-mail address: hogino@hsp.ncvc.go.jp (H. Ogino).

1010-7940/$ – see front matter © 2005 Elsevier B.V. All rights reserved.
doi:10.1016/j.ejcts.2005.10.040

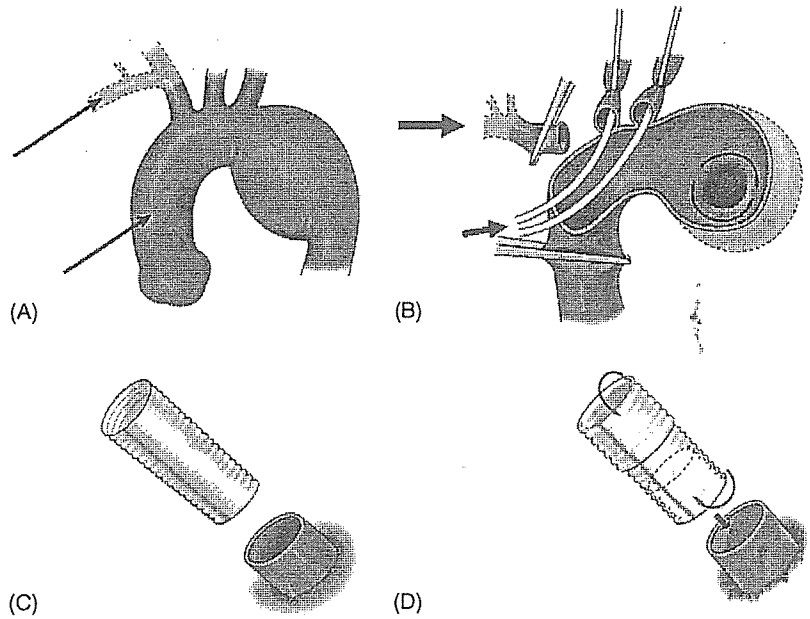

Fig. 1. Total arch replacement using selective cerebral perfusion and stepwise distal anastomosis. (A) Distal arch aneurysm: black arrows show cannulation sites on the right axillary artery and the ascending aorta for cardiopulmonary bypass. (B) Brain protection with antegrade selective cerebral perfusion (SCP): large (right axillary artery perfusion) and small (left common carotid and left subclavian artery perfusion) arrows show SCP. The descending aorta was divided from the inside through the aneurysm. (C) An invaginated tube graft was inserted into the descending aorta. (D) Recent refined technique (mini-elephant trunk technique): 2–3 cm of the proximal end was left without invagination so as to reinforce the anastomosis from the inside by a 'sandwich' technique with the outside Teflon felt strip. The distal end was also tucked inside to shorten the length of the graft, in order to prevent dislodge of the mural atheroma.

Rewarming was then initiated. The proximal anastomosis was done above the sinotubular junction. Finally, the LCCA and the BCA were reconstructed (Fig. 2C). The RAxA perfusion was discontinued. In recent cases, our stepwise technique was refined to reinforce the anastomosis and prevent bleeding from the anastomosis (Fig. 1D). In making the stepwise graft, 2–3 cm of the proximal end was left without invagination so as to reinforce the anastomosis from the inside by a 'sandwich' technique with the Teflon felt strip. We call this 'mini-elephant trunk technique'. Coronary artery bypasses grafting in 23, aortic valve replacement in one, and mitral valve plasty in one were also performed.

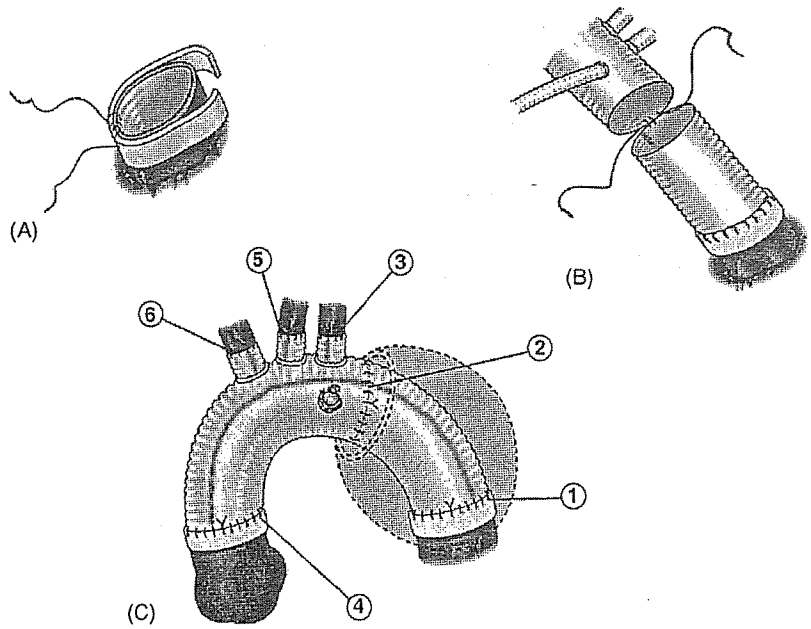

Fig. 2. Stepwise distal anastomosis. (A) Stepwise distal anastomosis with the reinforcement of outside Teflon felt strip using a running suture. (B) The distal end of the inserted graft was extracted and a quadrifurcated arch graft was connected to this end. (C) Total arch replacement using a stepwise anastomosis: the numbers show the turn of anastomosis.

3. Results

The median duration of lower body circulatory arrest, SCP, CPB, and surgery were 68, 147, 209, and 415 min, respectively. The median transfusion volume was 2400 ml. There were three hospital deaths (2.5%) from perioperative myocardial infarction, low cardiac output with bowel necrosis, and mediastinitis. Two patients (1.7%) developed permanent neurological dysfunction (small stroke), and three patients (2.5%) suffered from transient cerebral deficits. Three patients (2.5%) required reentry for bleeding. In none of them, bleeding from the distal anastomosis was found. Other complications occurred: low cardiac output in 5.0%, respiratory failure in 10.0%, renal failure in 3.3%, hepatic failure in 0.8%, bowel necrosis in 1.7%, and sepsis in 0.8%.

4. Discussion

The most common approach for arch to distal arch aneurysms is currently through median sternotomy [1–4]. This approach aims to provide cerebral and cardiac safety. However, the distal anastomosis tends to be difficult because of poor, distant, and limited view [6,7]. In our technique, the arch aneurysm is not incised to prevent injury to the nerves and lung. Through the aneurysm, the descending aorta is divided and the distal anastomosis takes place. Subsequently, the surgical view is limited. Furthermore, bleeding from this anastomosis is a major concern. We have therefore evolved a novel stepwise technique, which made the distal anastomosis around the hilum feasible in our experience.

The end of the descending aorta is often fragile with much atherosclerosis. Even with the stepwise technique, we experienced bleeding from the anastomosis in seven patients. The stepwise technique was therefore refined by the "mini-elephant trunk". With this refinement, we have not experienced any major bleeding from the distal anastomosis.

The stepwise technique has some drawbacks. Graft insertion carries a risk of dislodging mural atheroma. We experienced one case of bowel necrosis. To prevent this problem, in the refined technique, the distal end was tucked inside to shorten the graft length. Graft insertion must be done carefully into the atheromatous descending aorta. Direct anastomosis of a short-length graft without graft insertion is a good alternative. Another disadvantage is the need for a graft–graft anastomosis, which is fortunately easy with a good view taking 5–10 min.

References

[1] Bachet J, Guilmet D, Goudot B, Dreyfus GD, Delentdecker P, Brodaty D, Dubois C. Antegrade cerebral perfusion with cold blood: a 13-year experience. Ann Thorac Surg 1999;67:1874–8.
[2] Kazui T, Washiyama N, Muhammad BA, Terada H, Yamashita K, Takinami M. Total arch replacement using aortic arch branched grafts with the aid of antegrade selective cerebral perfusion. Ann Thorac Surg 2000;70(1):3–8.
[3] Kazui T, Washiyama N, Muhammad BA, Terada H, Yamashita K, Takinami M. Improved results of atherosclerotic arch aneurysm operations with a refined technique. J Thorac Cardiovasc Surg 2001;121(3):491–9.
[4] Kazui T, Yamashita K, Washiyama N, Terada H, Bashar AH, Suzuki T, Ohkura K. Usefulness of antegrade selective cerebral perfusion during aortic arch operations. Ann Thorac Surg 2002;74(5):S1806–9.
[5] Takamoto S, Okita Y, Ando M, Morota T, Handa N, Kawashima Y. Retrograde cerebral circulation for distal aortic arch surgery through a left thoracotomy. J Card Surg 1994;9(5):576–82 [discussion 582–3].
[6] Ogino H, Ueda Y, Sugita T, Matsuyama K, Matsubayashi K, Nomoto T, Yoshioka T. Aortic arch repairs through three different approaches. Eur J Cardiothorac Surg 2001;19(1):25–9.
[7] Westaby S, Katsumata T. Proximal aortic perfusion for complex arch and descending aortic disease. J Thorac Cardiovasc Surg 1998;115:162–7.
[8] Numata S, Ogino H, Sasaki H, Hanafusa Y, Hirata M, Ando M, Kitamura S. Total arch replacement using antegrade selective cerebral perfusion with right axillary artery perfusion. Eur J Cardiothorac Surg 2003;23(5):771–5.

Journal of Thrombosis and Haemostasis, 3: 2315–2323

ORIGINAL ARTICLE

Impaired platelet function in a patient with $P2Y_{12}$ deficiency caused by a mutation in the translation initiation codon

M. SHIRAGA,* S. MIYATA,† H. KATO,* H. KASHIWAGI,* S. HONDA,* Y. KURATA,‡ Y. TOMIYAMA* and Y. KANAKURA*

**Department of Hematology and Oncology, Graduate School of Medicine C9, Osaka University, Osaka, Japan; †Division of Blood Transfusion Medicine, National Cardiovascular Center, Osaka, Japan; and ‡Department of Blood Transfusion, Osaka University Hospital, Osaka, Japan*

To cite this article: Shiraga M, Miyata S, Kato H, Kashiwagi H, Honda S, Kurata Y, Tomiyama Y, Kanakura Y. Impaired platelet function in a patient with $P2Y_{12}$ deficiency caused by a mutation in the translation initiation codon. *J Thromb Haemost* 2005; 3: 2315–23.

Summary. In this study, we have identified a patient (OSP-1) with a congenital $P2Y_{12}$ deficiency showing a mild bleeding tendency from her childhood and examined the role of $P2Y_{12}$ in platelet function. At low concentrations of agonists OSP-1 platelets showed an impaired aggregation to several kinds of stimuli, whereas at high concentrations they showed a specifically impaired platelet aggregation to adenosine diphosphate (ADP). ADP normally induced platelet shape change and failed to inhibit PGE_1-stimulated cAMP accumulation in OSP-1 platelets. Molecular genetic analysis revealed that OSP-1 was a homozygous for a mutation in the translation initiation codon (ATG to AGG) in the *P2Y*$_{12}$ gene. Heterologous cell expression of wild-type or mutant $P2Y_{12}$ confirmed that the mutation was responsible for the deficiency in $P2Y_{12}$. OSP-1 platelets showed a markedly impaired platelet spreading onto immobilized fibrinogen. Real-time observations of thrombogenesis under a high shear rate (2000 s^{-1}) revealed that thrombi over collagen were small and loosely packed and most of the aggregates were unable to resist against high shear stress in OSP-1. Our data suggest that secretion of endogenous ADP and subsequent $P2Y_{12}$-mediated signaling are critical for platelet aggregation, platelet spreading, and as a consequence, for stabilization of thrombus.

Keywords: $\alpha_{IIb}\beta_3$, initiation codon, mutation, $P2Y_{12}$ deficiency, platelets, thrombogenesis.

Introduction

Platelets play a crucial role not only in a hemostatic plug formation, but also in a pathologic thrombus formation, particularly within atherosclerotic arteries subjected to high shear stress [1,2]. As an initial step in thrombogenesis, platelets adhere to exposed subendothelial matrices such as von Willebrand factor (VWF) and collagen, then become activated and aggregate to each other. These processes are primarily mediated by platelet surface glycoproteins such as GPIb-IX-V, $\alpha_2\beta_1$, GPVI, and $\alpha_{IIb}\beta_3$ (GPIIb-IIIa) [3,4]. In addition, several mediators such as adenosine diphosphate (ADP), thromboxane A_2, and thrombin cause further platelet activation and recruitment of circulating platelets to the injury sites through activation of $\alpha_{IIb}\beta_3$ and subsequent binding of VWF and fibrinogen.

Recent studies have demonstrated a critical role for ADP in arterial thrombogenesis [5–7]. ADP is actively secreted from platelet dense granules on platelet activation and is passively released from damaged erythrocytes and endothelial cells. Platelets possess at least two major G protein-coupled ADP receptors that are largely responsible for platelet responses to ADP: $P2Y_1$ and $P2Y_{12}$ [6]. $P2Y_1$ is the G_q-coupled receptor responsible for mediating platelet shape change and reversible platelet aggregation through intracellular calcium mobilization [8,9], whereas $P2Y_{12}$ is the G_i-coupled receptor responsible for mediating inhibition of adenylyl cyclase and sustained platelet aggregation [10–12]. $P2Y_{12}$ is the therapeutic target of efficacious antithrombotic agents, such as ticlopidine, clopidogrel, and AR-C compounds [5,6], and its congenital deficiency results in a bleeding disorder [13,14]. The analyses of patients with $P2Y_{12}$ deficiency as well as $P2Y_{12}$-null mice would provide more precise information about the role of $P2Y_{12}$ in platelet function than those using $P2Y_{12}$ inhibitors. To date, four different families with a defect in the expression or the function of $P2Y_{12}$ have been characterized [10,13–16]. In this study, we have described a patient with the congenital $P2Y_{12}$ deficiency due to a homozygous mutation in the translation initiation codon and analyzed the role of $P2Y_{12}$ in platelet aggregation, platelet spreading onto immobilized fibrinogen, and thrombogenesis on a type I collagen-coated surface under a high shear rate. Our present data have demonstrated a crucial role of $P2Y_{12}$ in various platelet functions.

Correspondence: Yoshiaki Tomiyama, Department of Hematology and Oncology, Graduate School of Medicine C9, Osaka University, 2-2 Yamadaoka, Suita Osaka 565-0871, Japan.
Tel.: +81 6 6879 3821; fax: +81 6 6879 3879; e-mail: yoshi@hp-blood.med.osaka-u.ac.jp

Received 2 November 2004, accepted 7 June 2005

Materials and methods

Patient history

The proband (OSP-1) is a 67-year-old Japanese female with a lifelong history of easy bruising. She (OSP-1) was born from non-consanguineous parents who had no hemorrhagic diathesis. Although she showed massive bleeding during delivery of her son, she had no history of transfusions. Patient OSP-1 showed normal platelet count, normal coagulation tests (prothrombin time and activated partial thromboplastin time) and slightly elevated plasma fibrinogen (398 mg dL^{-1}). Ivy bleeding time of the patient was consistently prolonged (> 15 min). Clot retraction by MacFarlane's method was normal (50%; normal values 40%–70%). Her son never suffered from a bleeding tendency. Informed consent for analyzing their platelet function and molecular genetic abnormalities was obtained from OSP-1, her husband and their son.

Preparation of platelet-rich plasma and washed platelet suspension

Platelet-rich plasma (PRP) for aggregation studies was prepared by a centrifugation of whole blood anticoagulated with citrate at 250 *g* for 10 min and then the platelet count was adjusted at 300×10^6 mL^{-1} by platelet-poor plasma. Washed platelets were prepared as previously described [17]. In brief, 6 volumes of freshly drawn venous blood from the patient, her husband, son or healthy volunteers were mixed with 1 volume of acid–citrate–dextrose (ACD; National Institutes of Health Formula A, NIH, Bethesda, MD, USA) and centrifuged at 250 *g* for 10 min to obtain PRP. After incubation with 20 ng mL^{-1} prostaglandin E1 (PGE_1; Sigma-Aldrich, St Louis, MO, USA) for 15 min, the PRP was centrifuged at 750 *g* for 10 min, washed three times with 0.05 mol L^{-1} isotonic citrate buffer containing 20 ng mL^{-1} PGE_1 and resuspended in an appropriate buffer.

Platelet aggregometry

Platelet aggregation using PRP was monitored by a model PAM-6C platelet aggregometer (Mebanix, Tokyo, Japan) at 37 °C with a stirring rate of 1000 r.p.m. as previously described [18]. Protease-activated receptor 1-activating peptide (PAR1 TRAP, SFLLRNPNDKYEPF) and adenosine 3′,5′-diphosphate (A3P5P) were purchased from Sigma-Aldrich Corp. $P2Y_{12}$ antagonist, AR-C6993MX (2-propylthio-D-fluoromethylene adenosine 5-triphosphate) was a kind gift from AstraZeneca (Loughborough, UK).

Flow cytometry and measurement of intracellular cAMP

Flow cytometric analysis using various monoclonal antibodies (mAbs) specific for platelet membrane glycoproteins was performed as previously described [19].

For measuring intracellular cAMP levels, samples of 200 μL of washed platelets (60×10^6) in Walsh buffer (137 mM of NaCl, 2.7 mM of KCl, 1.0 mM of $MgCl_2$, 3.3 mM of NaH_2PO_4, 3.8 mM of HEPES, 0.1% of glucose, 0.1% of BSA, pH 7.4) were incubated with 1 μmol L^{-1} PGE_1 for 15 min, and then platelets were stimulated with ADP or epinephrine. After incubation for 15 min, total cellular cAMP levels were measured using the Biotrak cAMP enzyme immunoassay system from Amersham Pharmacia Biotech (Piscataway, NJ, USA).

Platelet adhesion assay

Adhesion study was performed as previously described [20]. In brief, non-treated polystyrene 10 cm dishes were coated with 100 μg mL^{-1} human fibrinogen in 5 mL of phosphate-buffered saline (PBS) at 4 °C overnight. After washing with PBS, dishes were blocked with PBS containing 1% of bovine serum albumin (BSA) for 90 min at 37 °C. Aliquots (1 mL) of washed platelets (25×10^6 mL^{-1}) were added to the fibrinogen-coated dishes and incubated at 37 °C. After incubation for 40 min, adherent platelets were fixed with 3.7% formaldehyde, permeabilized with 0.1% Triton X-100 and stained with TRITC-conjugated phalloidin. Platelet morphology and degrees of spreading were determined by fluorescence microscopy (Olympus, Tokyo, Japan).

Platelet thrombus formation under flow conditions

The real-time observation of mural thrombogenesis on a type I collagen-coated surface under a high shear rate (2000 s^{-1}) was performed as previously described [21]. In brief, type I collagen-coated glass coverslips were placed in a parallel plate flow chamber (rectangular type; flow path of 1.9-mm width, 31-mm length, and 0.1-mm height). The chamber was assembled and mounted on a microscope (BX60; Olympus, Tokyo, Japan) equipped with epifluorescent illumination (BX-FLA; Olympus) and a charge-coupled device (CCD) camera system (U-VPT-N; Olympus). Whole blood containing mepacrine-labeled platelets obtained from OSP-1 or control subjects was aspirated through the chamber by a syringe pump (Model CFV-3200, Nihon Kohden, Tokyo, Japan) at a constant flow rate of 0.285 mL min^{-1}, producing a wall shear rate of 2000 s^{-1} at 37 °C.

Amplification and analysis of platelet RNA

Total cellular RNA of platelets was isolated from 20 mL of whole blood, and $P2Y_1$ or $P2Y_{12}$ mRNA was specifically amplified by reverse transcription-polymerase chain reaction (RT-PCR), as previously described [22]. The following primers were constructed based on the published sequence of $P2Y_{12}$ cDNA and used for the first round PCR for $P2Y_{12}$ cDNA: Y12F1, 5′-GGCTGCAATAACTACTACTTACT-GG-3′ [sense, nucleotide(nt) −74 to −50]; Y12R4, 5′-CAGGA-CAGTGTAGAGCAGTGG-3′ (antisense, nt 85 to 105) [10].

Allele-specific restriction enzyme analysis (ASRA)

Genomic DNA was isolated from mononuclear cells using SepaGene kit (Sanko Junyaku Co Ltd, Tokyo, Japan). Amplification of the region around the initiation codon of the $P2Y_{12}$ gene was performed by using primers *Bsr*DI-GF, 5′-CTTTTGTTCTCTAGGTAACCAACAAGCAA-3′ (sense, the mismatched base is underlined), and Y12R4 (antisense described above) using 250 ng of DNA as a template. These primers can be found in GenBank accession no. AC024886.20 and the sense primer corresponds to 127558–127585. PCR products were then digested with restriction enzyme *Bsr*DI. The resulting fragments were electrophoresed in a 6% polyacrylamide gel.

Construction of $P2Y_{12}$ expression vectors and cell transfection

The full-length cDNA of wild-type (WT) and mutant $P2Y_{12}$ was amplified by RT-PCR using primers Y12-*Hin*dIII-F, 5′-GAATTCAAGCTTCAAGAAATGCAAGCCGTCGACA-ACCTC-3′ (sense, nt −6 -21 for WT, *Eco*RI and *Hin*dIII sites introduced at the 5′ end were underlined) or Y12-*Hin*dIII-F2, 5′-GAATTCAAGCTTCAAGAAAGGCAAGCCGTCGAC-AACCTC-3′ (sense, nt −6 −21 for mutant), and Y12H-Not-R, 5′-TCTAGAGCGGCCGCTCAATGGTGATGGTGATGA-TGCATTGGAGTCTCTTCATT-3′ (antisense, nt 1012–1029, His × 6 were introduced before stop codon, *Not*I and *Xba*I sites introduced at the 5′ end were underlined). The amplified fragments were digested with *Hin*dIII and *Not*I, and the resulting 1059-bp fragments (nt −9 −1050) were extracted using QIAquick gel extraction kit (Qiagen, GmbH, Germany). These fragments were inserted into the pcDNA3 (Invitrogen, San Diego, CA, USA) digested with *Hin*dIII and *Not*I. The fragments inserted were characterized by sequence analysis to verify the absence of any other substitutions and the proper insertion of the PCR cartridge into the vector.

A total of 10 μg of WT or mutant $P2Y_{12}$ construct was transfected into human embryonic kidney 293 cells (HEK293 cells, 10^6 cells) using the calcium phosphate method as previously described [22]. Transfectants were lyzed by 1% Triton X-100 PBS containing protease inhibitors 2 days after transfection, and proteins were separated by 7.5% SDS-PAGE. After transferred onto a PVDF membrane, expressed proteins were detected by rabbit anti-His tag antibody.

Results

Platelet aggregation studies

We first examined the expression of platelet membrane glycoproteins in OSP-1 by flow cytometry. The patient's platelets (OSP-1 platelets) normally express GPIb-IX, $\alpha_{IIb}\beta_3$ (GPIIb-IIIa), $\alpha_2\beta_1$, and CD36 (data not shown). Fig. 1 shows platelet aggregation of PRP in response to various agonists. The aggregation of OSP-1 platelets induced by 20 μM of ADP was markedly impaired with only a small and transient

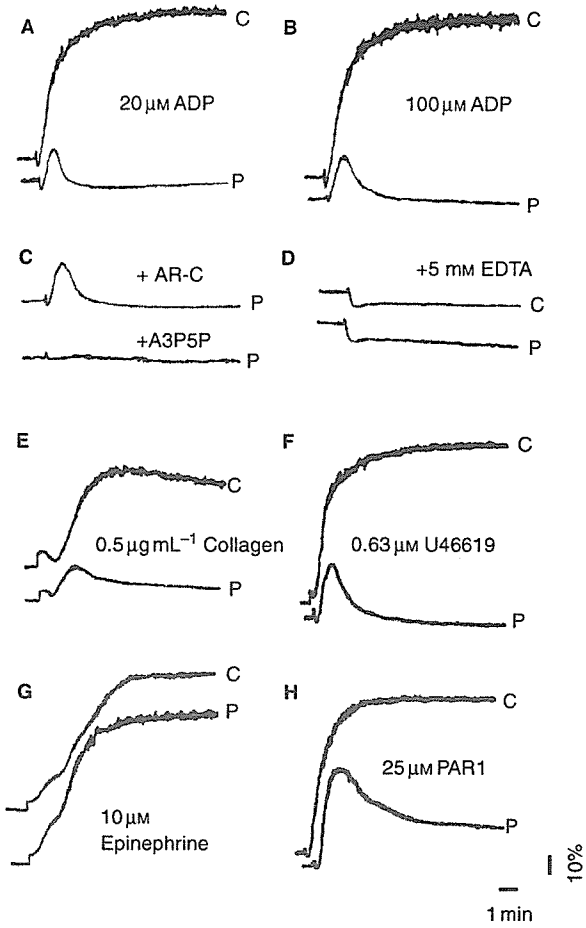

Fig. 1. Platelet aggregation induced by various agonists. Platelet aggregation was induced by various agonists in citrated PRP from patient OSP-1 (labeled 'P') or a control subject (labeled 'C'). Agonists used are (A) 20 μM of ADP, (B) 100 μM of ADP, (C) 20 μM of ADP in the presence of 1 μM of AR-C69931MX ('AR-C'), a specific $P2Y_{12}$-antagonist, or 1 mM of A3P5P ('A3P5P'), a specific $P2Y_1$-antagonist, (D) 20 μM of ADP in the presence of 5 mM of EDTA, (E) 0.5 μg mL^{-1} of collagen, (F) 0.63 μM of U46619, (G) 10 μM of epinephrine, and (H) 25 μM of PAR1-TRAP.

aggregation (Fig. 1A), and the aggregation was still impaired even at 100 μM of ADP (Fig. 1B). As compared with control platelets, the aggregation of OSP-1 platelets was also impaired with a transient aggregation in response to low concentrations of collagen (0.5 μg mL^{-1}, Fig. 1E), U46619 (0.63 μM, Fig. 1F), or PAR1 TRAP (25 μM, Fig. 1H). In response to 1.3 mg mL^{-1} ristocetin (not shown) or 10 μM of epinephrine (Fig. 1G), OSP-1 platelets aggregated normally. When OSP-1 platelets were stimulated with 20 μM of ADP in the presence of 5 mM of EDTA, the light transmission decreased equivalent to control platelets suggesting that OSP-1 platelets changed shape normally (Fig. 1D). We then examined effects of ADP receptor antagonists on the aggregation of OSP-1 platelets induced by 20 μM of ADP. A total of 1 mM of A3P5P, a specific $P2Y_1$ antagonist, abolished the residual response of OSP-1 platelets to ADP, whereas 1 μM of AR-C69931MX, a specific $P2Y_{12}$

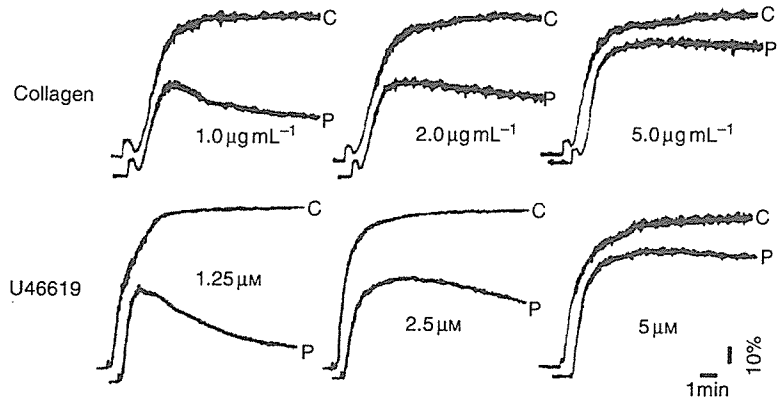

Fig. 2. Platelet aggregation induced by collagen or U46619 at various concentrations. Platelet aggregation in citrated PRP from patient OSP-1 (labeled 'P') or a control subject (labeled 'C') was induced by various concentrations of collagen or U46619. At high concentrations of collagen or U46619, OSP-1 platelets aggregate almost normally.

antagonist, did not induce an additional inhibition on the platelet aggregation (Fig. 1C). These data suggest that the impaired response of the patient's platelets may be due to an abnormality in signaling evoked by ADP and that $P2Y_{12}$-mediated signaling rather than $P2Y_1$-mediated signaling may be completely defective in patient OSP-1.

We also examined the aggregation of OSP-1 platelets induced by higher concentrations of agonists. As shown in Fig. 2, the aggregation response of OSP-1 platelets improved as the concentrations of agonists increased, and they aggregated almost normally in response to high concentrations of collagen (5 μg mL^{-1}), U46619 (5 μM), or PAR1 TRAP (100 μM) (not shown). In addition, we confirmed that 1 μM of AR-C69931MX conferred essentially the same defect on the aggregation of control platelets in response to U46619 as that of OSP-1 platelets and did not further inhibit OSP-1 platelet aggregation induced by 5 μg mL^{-1} of collagen, 5 μM of U46619, or 100 μM of PAR1 TRAP (data not shown). These data indicated that at high concentrations of agonists OSP-1 platelets showed the specifically impaired aggregation to ADP.

Effect of ADP on PGE_1-stimulated cAMP accumulation in platelets

To determine whether $P2Y_{12}$-mediated signaling is specifically impaired, we examined an inhibitory effect of ADP on 1 μM of PGE_1-stimulated cAMP accumulation in platelets from the patient, her husband, their son, and healthy unrelated controls. ADP inhibited intracellular cAMP levels in platelets from the patient's husband, son and healthy unrelated controls (not shown) by approximately 80%, whereas the inhibition was only 15% in the patient's platelets (Fig. 3). In contrast to ADP, epinephrine normally inhibited cAMP accumulation in platelets from the patient as well as her husband and son. These results strongly suggest that the defect could be due to an abnormality in G_i coupling ADP receptor, $P2Y_{12}$.

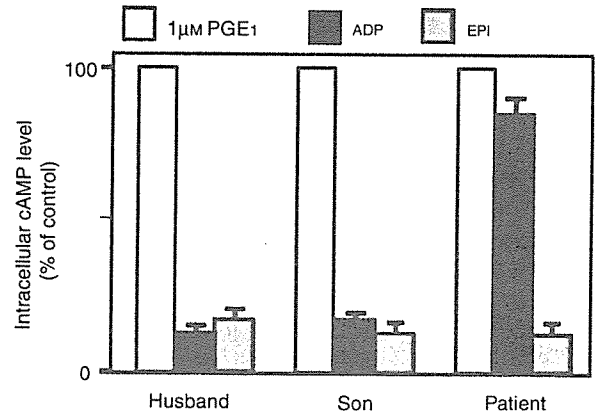

Fig. 3. Effect of ADP or epinephrine on the inhibition of PGE_1-induced cAMP accumulation in platelets. Washed platelets from patient OSP-1, husband or son were incubated with 1 μM of PGE_1 for 15 min and stimulated with 20 μM of ADP or 10 μM of epinephrine. Intracellular cAMP levels were expressed as a percent of cAMP levels in the absence of agonists. Results in OSP-1 are the mean of two experiments.

Nucleotide sequence analysis of cDNA and genomic DNA of $P2Y_{12}$

To reveal a molecular genetic defect in OSP-1, we analyzed the entire coding regions of both $P2Y_1$ and $P2Y_{12}$ cDNAs amplified from platelet mRNA by RT-PCR. A single nucleotide substitution (T → G) was identified within the translation initiation codon (ATG → AGG) in the patient's $P2Y_{12}$ cDNA (Fig. 4A). This substitution was also confirmed by reverse sequencing. No other nucleotide substitutions were detected within the coding region of either $P2Y_{12}$ or $P2Y_1$ cDNA from the patient. OSP-1 appeared homozygous for the substitution, and the substitution was not detected in 20 control subjects.

Nucleotide sequence analysis of PCR fragments from the patient's genomic DNA also suggested the homozygosity of the substitution (data not shown). To further confirm the homo-

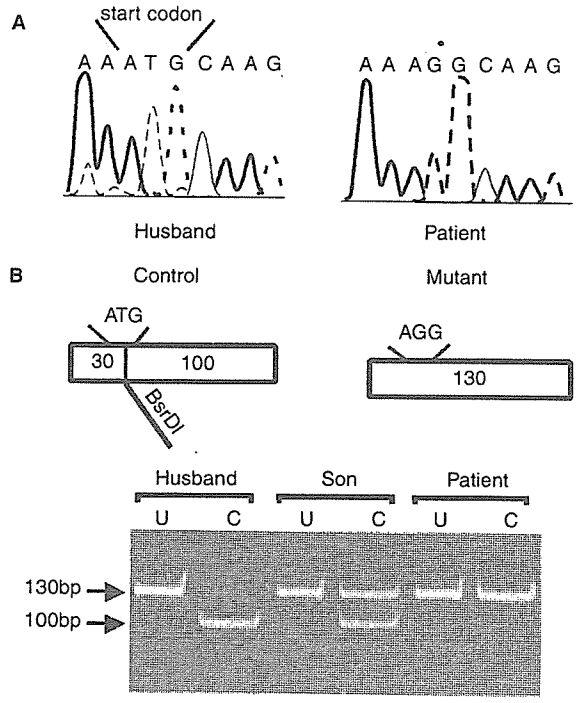

Fig. 4. Sequence analysis of $P2Y_{12}$ cDNA and restriction enzyme analysis of the $P2Y_{12}$ gene. (A) cDNA obtained by RT-PCR from platelet mRNA was analyzed by sequencing using a sense primer Y12F1. (B) PCR was performed to generate 130-bp fragments including initiation codon of $P2Y_{12}$ as described in Materials and methods. Undigested (U) or digested (C) PCR products with *Bsr*DI were analyzed on a 6% polyacrylamide gel. In patient OSP-1, the T → G mutation at position 2 abolishes a *Bsr*DI restriction site.

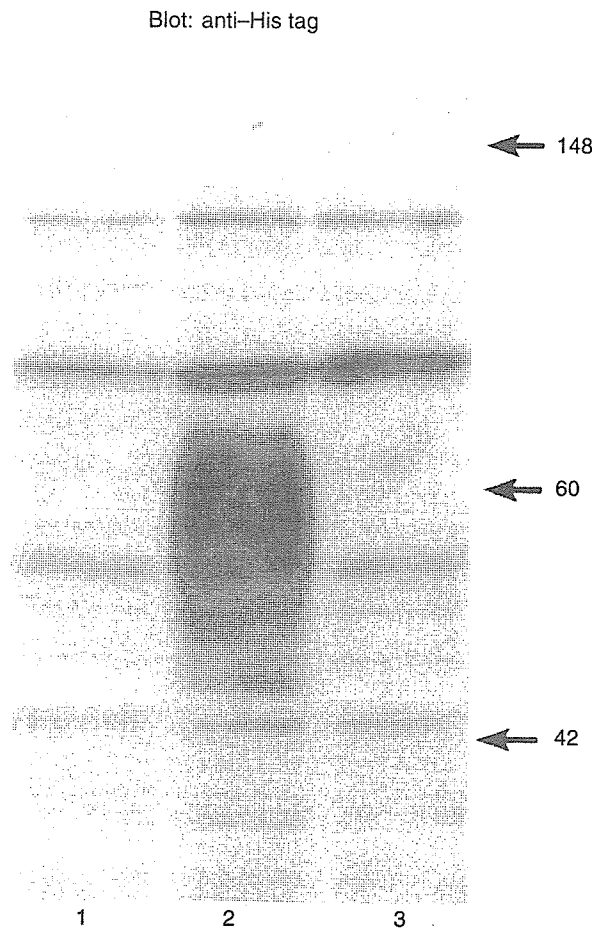

Fig. 5. Expression of $P2Y_{12}$ in HEK293 cells transfected with WT or mutant His-tag attached $P2Y_{12}$. Wild-type or mutant $P2Y_{12}$ construct was transfected into HEK293 cells using the calcium phosphate method. Transfectants were lyzed by 1% Triton X-100 PBS containing protease inhibitors 2 days after transfection. Cell lysates from mock transfectant (lane 1), cells transfected with WT $P2Y_{12}$ (lane 2) or mutant $P2Y_{12}$ (lane 3) were separated by 7.5% SDS-PAGE, and immunoblot was performed by anti-His-tag antibodies.

zygosity, allele-specific restriction enzyme analysis (ASRA) was performed. The region around the initiation codon of the $P2Y_{12}$ gene was amplified by PCR using primers *Bsr*DI-GF and Y12R4. A restriction site for *Bsr*DI would be abolished by the T → G substitution. As shown in Fig. 4B, ASRA clearly indicated that the patient and her son were homozygous and heterozygous for the substitution, respectively. These results also confirm that the substitution is inheritable.

Heterologous cell expression of WT and mutant $P2Y_{12}$

As the substitution at the translation initiation codon might induce an alternative translation starting at downstream ATGs leading to an expression of shorter form of $P2Y_{12}$, we decided to investigate effects of the substitution found in the patient on the expression of $P2Y_{12}$. Expression vectors encoding WT and mutant $P2Y_{12}$ in which His-tag was attached at the C-terminal portion of $P2Y_{12}$ were constructed as described in the Materials and methods. Wild-type or mutant $P2Y_{12}$ construct was transfected into HEK 293 cells, and then expressed proteins were analyzed 48 h after transfection in an immunoblot assay employing anti-His antibodies. As shown in Fig. 5, WT $P2Y_{12}$ protein with an apparent molecular weight of ~60 KDa was expressed in 293 cells as a His-tag-positive protein. In sharp contrast, the mutant $P2Y_{12}$-expression vector failed to express any His-tag-positive protein. These results provide strong evidence that the T → G substitution at the translation initiation codon of $P2Y_{12}$ cDNA is responsible for the $P2Y_{12}$ deficiency.

Platelet spreading on immobilized fibrinogen

As it has been well documented that release of endogenous ADP is required for full platelet spreading onto immobilized fibrinogen [23], we next analyzed the patient's platelet spreading in order to evaluate the role of $P2Y_{12}$. Control platelets adhered to fibrinogen underwent morphological changes ranging from filopodia protrusion to complete spreading, and 50.5% ± 21.3% of the adherent platelets spread ($n = 3$) (Fig. 6A). In sharp contrast, the patient's platelets showed an

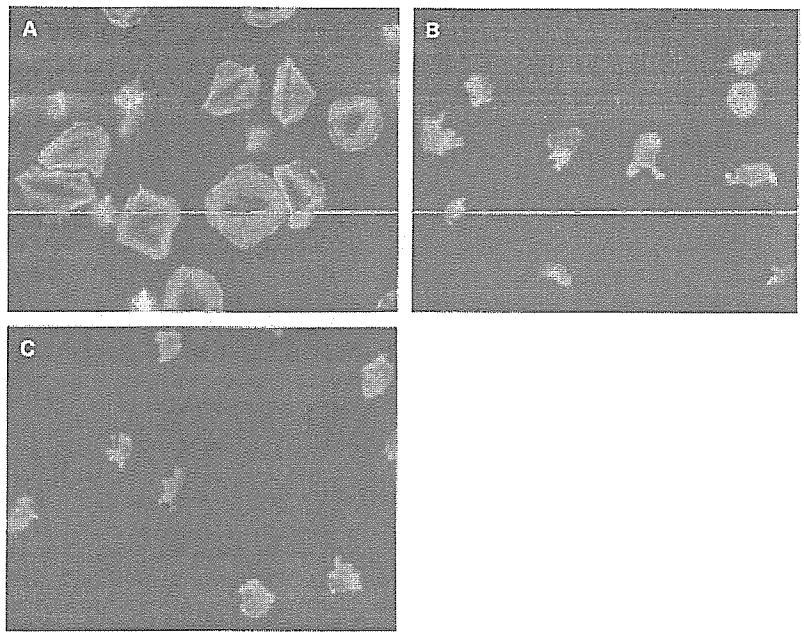

Fig. 6. Platelet spreading on immobilized fibrinogen. (A,B) Washed platelets from a control subject were applied onto fibrinogen-coated polystyrene dishes and incubated at 37 °C for 40 min without any inhibitor (A) or with 1 μM of AR-C69931MX (B). (C) Washed platelets from the patient were applied onto fibrinogen-coated polystyrene dishes and incubated at 37 °C for 40 min without any inhibitor. Adherent platelets were then fixed, permeabilized and stained with TRITC-conjugated phalloidin. Platelet morphology was analyzed by fluorescence microscopy.

impaired spreading and only 2.3% ± 1.4% of the adherent platelets spread ($n = 3$, $P < 0.001$, Fig. 6C). Similar results were obtained with control platelets in the presence of 1 μM of AR-C69931MX (6.2% ± 2.2%, $n = 3$, $P < 0.001$, Fig. 6B). In addition, 1 mM of A3P5P also markedly inhibited platelet spreading ($n = 3$, 10.1% ± 2.2%, $P < 0.001$, not shown). These results suggest that both $P2Y_{12}$ and $P2Y_1$ are necessary for platelet spreading.

Platelet-thrombus formation on immobilized collagen under flow conditions

To investigate the role of $P2Y_{12}$ in thrombus formation, we observed the real-time process of mural thrombogenesis on a type I collagen-coated surface under flow conditions with high shear rate (2000 s^{-1}) using the whole blood from OSP-1. Real-time observation revealed that thrombi formed on type I collagen were unstable. As platelet aggregates of the patient were loosely packed each other and unable to resist against high shear stress, most of the aggregates at the apex of the thrombi came off the thrombi constantly. On the other hand, most of thrombi formed by control platelets were densely packed with higher fluorescent intensity and were stable with constant growth during observation (Video 1 and 2).

As shown in Fig. 7A, the area covered with patient platelets after 7 min of flow was greater than that of control platelets (91.8% ± 0.3% vs. 82.2% ± 1.4%, $n = 3$, $P < 0.01$). However, thrombi formed by OSP-1 platelets were loosely packed, whereas thrombi were large and densely packed in controls. The overall fluorescent intensity of thrombi of OSP-1 platelets was lower than that of control platelets. Three-dimensional analysis revealed the striking difference in size and shape of individual thrombus formed after 10 min between the patient and control platelets (Fig. 7B). Thrombi formed by control platelets were large in size, clearly edged and surrounded by thrombus-free areas. On the other hand, individual thrombus formed by patient platelets was mostly small and appeared to be a thin layer of platelet aggregates. Thrombus height at the plateau phase was 10.2 ± 0.4 μm, which was less than half of controls (21.2 ± 0.4 μm).

Discussion

$P2Y_{12}$ coupled with $G\alpha_i$, primarily with $G\alpha_{i2}$, consists of 342 amino acid residues with seven transmembrane domains (TM), and its deficiency is responsible for congenital bleeding diathesis [10–16]. To date, five mutations responsible for a defect in the expression or the function of $P2Y_{12}$ in four different families have been demonstrated [10,15,16]. Patient ML possessed a mutation consisting of a two nucleotide deletion at amino acid 240 (near the N-terminal end of TM6), which would lead to a premature termination of $P2Y_{12}$ [10,14]. A two nucleotide deletions at amino acid 98 (next to the N-terminal end of TM3) and a single nucleotide deletion occurring just beyond TM3 were identified in other two families, both of which would lead to a premature termination of $P2Y_{12}$ [13,15]. However, in these reports expression studies had not been performed to show the direct association between these mutations and the $P2Y_{12}$ deficiency [10,15]. Patient AC, whose platelets expressed dysfunctional $P2Y_{12}$ with normal

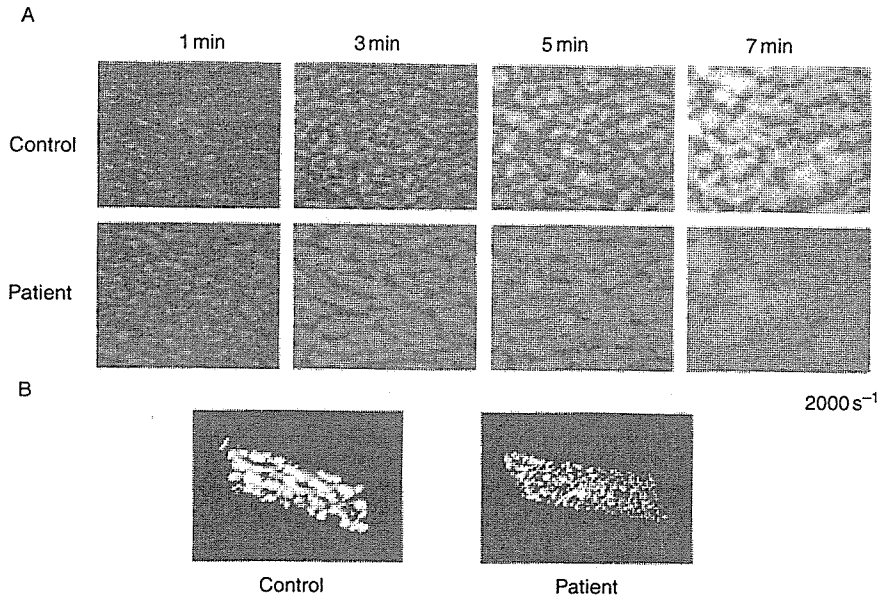

Fig. 7. Thrombus formation on immobilized collagen under flow conditions. (A) Whole blood containing mepacrine-labeled platelets obtained from the patient or control subjects was aspirated through a chamber with type I collagen-coated coverslips. Thrombi formed under a high shear rate (2000 s^{-1}) at indicated time points were observed using a microscope equipped with epifluorescent illumination and a CCD camera system. (B) Three-dimensional structure of thrombi formed after 10 min flow by platelets from the patient or a control subject was analyzed.

binding capacity of 2-methylthioadenosine 5′-diphosphate (2MeS-ADP), was compound heterozygous for Arg256 → Gln in TM6 and for Arg265 → Trp in the third extracellular loop of P2Y$_{12}$. Platelets from patient AC showed an increased platelet aggregation at high dose ADP compared with low dose ADP, suggesting the presence of residual receptor function [16]. In this study, we described a patient (OSP-1) with congenital bleeding diathesis bearing a novel homozygous mutation within the translation initiation codon (ATG → AGG) of the P2Y$_{12}$ gene. Consistent with previous studies, the aggregation of OSP-1 platelets with P2Y$_{12}$ deficiency was impaired to various agonists such as collagen, U46619, and PAR1 TRAP at low concentrations, but almost normal at high concentrations [11–14]. These findings confirmed the critical role of P2Y$_{12}$-mediated signaling evoked by endogenous ADP in platelet aggregation induced by low concentrations of agonists. In contrast to patient AC with residual P2Y$_{12}$-mediated signaling, the impaired platelet aggregation in OSP-1 in response to ADP was neither improved even at 100 μM of ADP stimulation nor reduced by adding 1 μM of AR-C69931MX, suggesting a complete loss of the P2Y$_{12}$ function. Family study confirmed that patient OSP-1 was homozygous for the mutation, and our expression study demonstrated that the mutation is responsible for the P2Y$_{12}$ deficiency.

A number of examples of mutations in the translation initiation codons have been demonstrated in various diseases [24]. Although some cases having mutations in the initiation codons did not express any related abnormal protein, Pattern *et al.* showed an abnormal Gα_s protein possibly synthesized as a result of initiation at downstream ATGs due to a mutation at an initiation codon (ATG → GTG) in patients with Albright's hereditary osteodystrophy [24,25]. In OSP-1, we detected the T → G mutation at position +2, and our expression study denied the possibility that the substitution might induce an alternative translation at downstream ATGs leading to an expression of shorter form of P2Y$_{12}$.

As to platelet spreading onto immobilized fibrinogen, OSP-1 platelets showed the impaired platelet spreading. Similarly, A3P5P inhibited the platelet spreading. It has been well documented that release of endogenous ADP is required for full platelet spreading onto immobilized fibrinogen [23], and Obergfell *et al.* [26] have demonstrated that the platelet spreading requires sequential activation of Src and Syk in proximately to $\alpha_{IIb}\beta_3$. In contrast to the ADP-induced platelet shape change shown in OSP-1 platelets in the platelet aggregometer, our data indicated that both P2Y$_{12}$ and P2Y$_1$ were necessary for the full spreading onto immobilized fibrinogen.

Employing clopidogrel or AR-C69931 MX as an inhibitor for P2Y$_{12}$, several studies examined the role of P2Y$_{12}$ in thrombogenesis under flow conditions [27–30]. However, some discrepancy between the studies was pointed out and non-specific effects of these inhibitors were not completely ruled out [28–30]. As patient OSP-1 was deficient in P2Y$_{12}$ as shown in this study, it would be informative to examine the real-time process of thrombogenesis on a type I collagen-coated surface under a high shear rate (2000 s^{-1}) employing whole blood obtained from OSP-1. Our data demonstrated that P2Y$_{12}$-deficiency led to the loosely packed thrombus and the impaired thrombus growth with enhancing adhesion to collagen, which was consistent with the study by Remijn *et al.* [30] employing patient ML's platelets. The increase in platelet adhesion to